# A complementarity model for closed-loop power converters

Valentina Sessa*, *Member, IEEE*, Luigi Iannelli†, *Senior Member, IEEE*, Francesco Vasca†, *Senior Member, IEEE*

*Corresponding author. Department of Engineering, University of Sannio, Piazza Roma 21, 82100 Benevento, Italy. phone: +390824305560, email: valentina.sessa@unisannio.it

†Department of Engineering, University of Sannio, Piazza Roma 21, 82100 Benevento, Italy. email: {luigi.iannelli, vasca}@unisannio.it

**Abstract**

At a certain level of abstraction power converters can be represented as linear circuits connected to diodes and controlled electronic switches. The evolutions of the electrical variables are determined by the state-dependent switchings, which complicate the mathematical modeling of controlled power converters. Differently from the complementarity models previously presented in the literature, the model proposed in this paper allows to represent as a linear complementarity system also closed-loop power converters, without requiring the a priori knowledge of the converter modes. A model construction procedure, not dependent on the specific converter topology, is presented. The discretization of the continuous-time model allows to formulate mixed linear complementarity problems for the computation of the control-to-output frequency response and the evolutions of both transient and steady-state currents and voltages. As illustrative examples Z-source, boost and buck DC–DC power converters under voltage-mode control and current-mode control operating both in continuous and discontinuous conduction modes are considered.

**Index Terms**

Circuit modeling; Closed loop systems; Switching circuits; DC–DC power conversion; Discrete time systems.

The manuscript has been submitted solely to this journal and is not published, in press, or submitted elsewhere.

## I. Introduction

THE typical averaged and switched models of power converters are based on construction procedures which depend on sequence of modes and operating conditions, [1], [2], [3], [4]. Consequently, the use of these models for the analysis of the closed-loop power converters requires the introduction of suitable simplifying assumptions, [5], [6].

Complementarity models, [7], represent an attractive solution to overcome some of these drawbacks. Recently they have been proposed as an useful framework for modeling linear circuits with diodes and ideal switches, [8], [9]. Indeed, the complementarity framework can be used to model a wide class of nonsmooth dynamical systems, such as mechanical systems with Coulomb friction, [10] and piecewise linear Lur'e systems, [11].

Such idea has been more specifically applied to power converters in [12]. Linear complementarity (LC) models have been proposed for modeling specific open-loop power converters topologies: single-phase diode bridges, [13], three-phase rectifiers, [14], switched capacitors, [15], resonant converters, [16]. Dealing with more general classes of power converters, the complementarity models proposed in [17] and [18] are constructed by considering the specific switches states and by assuming the a priori knowledge of the power converter configuration at each switching time instant. A strong limitation of the models proposed in [8], [12] and [19] is that they require switching of the sets (*cones*) of the complementarity variables. Unfortunately this property does not allow to obtain the models of controlled power converters in a manageable closed form. An alternative approach with fixed cones and characteristics depending on some external forcing variable is presented in [20]: the switch model is a signum characteristic having the switch current as the argument and whose amplitude is a piecewise linear function of an external control voltage. In [21] transistors are modeled within the complementarity framework, but the analysis is limited to static circuits. In [13] the switches are modeled by means of equivalent finite resistors representing the ON (conducting) and OFF (blocking) states determined by the signum of an external voltage signal. That model cannot be easily generalized to the case of zero conducting and infinite blocking equivalent resistances.

The model proposed in this paper is able to represent in an LC explicit form the large signal dynamics of closed-loop power converters. The complementarity model is simple to be built and captures all modes of the converter, without enumerating them, nor assuming the a priori knowledge of the sequence of modes and of the switching time instants. Such LC model is shown to be useful for the computation of the control-to-output frequency response, which is a crucial issue for controlled power converters so as analyzed in [16], [22] and the references therein. Moreover the proposed LC model of closed-loop power converters allows to obtain directly the closed-loop steady-state behaviour, which is often a nontrivial task so as in the case of LCC resonant converters, [23], [24] and modular multilevel converters, [25], [26].

The rest of the paper is organized as follows. In Section II the static LC models corresponding to the ideal diode and the controlled switches characteristics are presented. The procedure for the construction of the dynamic LC model of a power converter, both in open-loop and closed-loop, is described in Section III. Section IV shows how this representation allows to compute the steady-state periodic oscillation as a solution of a mixed LC problem

derived from the discretized closed-loop system. In Section V the approach used for the steady-state solution is applied for the computation of the control-to-output frequency response for a Z-source converter [27] whereas the uniqueness of the steady-state solution is guaranteed by the passivity hypothesis. In Section VI the usefulness of the proposed technique for the computation of transient and steady-state solutions of closed-loop power converters is numerically demonstrated by considering current-controlled and voltage-controlled boost DC–DC power converters with stable and unstable periodic solutions [4], [28] and a closed-loop buck DC–DC converter which exhibits multiple solutions [29]. Section VII concludes the paper.

## II. Complementarity models of electronic devices

The idealized voltage–current characteristics of electronic devices can be represented by means of static LC models. To show this, let us introduce the definition of a *mixed* LC problem, [30]. Given a vector $q \in \mathbb{R}^r$, a matrix $M \in \mathbb{R}^{r\times r}$ and lower and upper bounds $l, u \in \mathbb{R}^r \cup \{-\infty, +\infty\}^r$, a mixed LC problem consists of finding $z \in \mathbb{R}^r$ such that

$$w - v = Mz + q \tag{1a}$$

$$0 \leqslant w \perp (z - l) \geqslant 0 \tag{1b}$$

$$0 \leqslant v \perp (u - z) \geqslant 0, \tag{1c}$$

where "$\perp$" represents the orthogonality symbol, i.e., $w \perp (z - l)$ stands for $w^\top (z - l) = 0$, and inequalities among vectors are meant componentwise. In the case $l = u$, the unique solution of (1) is $z = l = u$. For $l \neq u$ the nonnegative variables $w$ and $v$ are complementary meaning that componentwise at least one of the two must be zero. The mixed LC problem is well-know in the mathematical programming theory, in fact it provides a natural setting for the Karush–Kuhn–Tucker conditions of a quadratic program with general equality and inequality constraints, [7].

When the lower bound $l$ is zero and the upper bound $u$ is infinity, we get $v = 0$ and the mixed LC problem becomes a *classical* LC problem with $w$ and $z$ being the usual complementarity variables. Then, given a vector $q \in \mathbb{R}^r$ and a matrix $M \in \mathbb{R}^{r\times r}$, a LC problem consists of finding $z$ such that

$$w = Mz + q \tag{2a}$$

$$0 \leqslant w \perp z \geqslant 0. \tag{2b}$$

It is well-known that an LC problem in the form (2) has a unique solution for all $q$ if and only if $M$ is a P-matrix, [7]. A matrix $M$ is called a P-matrix if all its principal minors are positive. According to the definition, every positive definite matrix is a P-matrix, but the converse is not true. If the matrix $M$ is only positive semidefinite, then the uniqueness of the LC problem solution cannot be proved, but it is possible to prove that among all solutions of the LC problem the least-norm one is unique, [31].

The LC framework can be used to represent idealized voltage–current characteristics of electronic devices. To this aim let us associate to (2) an 'output' equation in the form

$$\varphi = Nz, \tag{3}$$

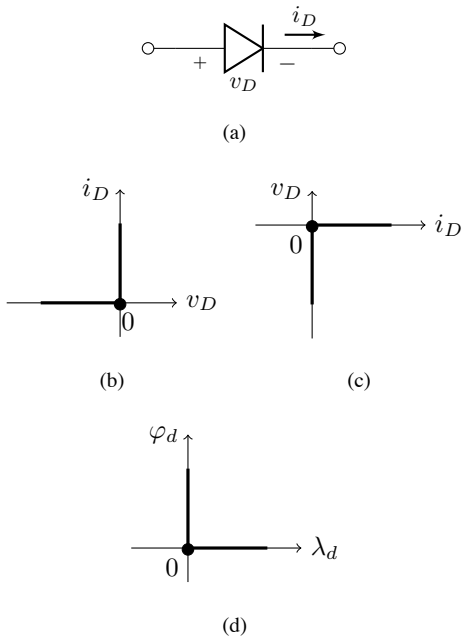


Fig. 1. Ideal diode: (a) symbol, (b) idealized voltage–current characteristic, (c) idealized current–voltage characteristic, (d) characteristic $(\varphi_d, \lambda_d)$ with input $\lambda_d = -v_D$ and output $\varphi_d = i_D$ or with input $\lambda_d = i_D$ and output $\varphi_d = -v_D$.

where $N$ is a real matrix of suitable dimensions. The expressions (2)–(3) can represent an LC *model* for a $(\varphi, \lambda)$ electronic device characteristic: the variable $\lambda$ can be interpreted as the input of the characteristic and enters into the LC problem if the vector $q$ depends linearly on it, and $\varphi$ can be seen as the corresponding output. As an example, let us consider the idealized piecewise linear diode characteristic shown in Fig.s 1(b)–1(c) and assume that the opposite of the diode voltage, say $\lambda_d = -v_D$, is the given input. Then the output variable of the diode model can be chosen as the diode current $\varphi_d = i_D$. By considering the resulting characteristic in Fig. 1(d) the diode characteristic can be represented with the following LC model

$$\varphi_d = z_d \tag{4a}$$

$$w_d = \lambda_d \tag{4b}$$

$$0 \leqslant w_d \perp z_d \geqslant 0. \tag{4c}$$

The equation (4a) is in the form (3) with $N = 1$ and (4b)–(4c) are in the form (2a)–(2b) with $M = 0$ and $q = \lambda_d$. Since $M$ is zero, the current $z_d$ which satisfies (4) for a given voltage $\lambda_d$ is not necessarily unique, while the least-norm solution must be unique. Indeed if $\lambda_d = 0$ then any $z_d \geqslant 0$ satisfies (4), but the least-norm solution ($z_d = 0$) is unique. Obviously (4) represents the ideal characteristic of a diode also if $\lambda_d = i_D$ and $\varphi_d = -v_D$, i.e., when the problem consists of finding a diode voltage $\varphi_d$ given the diode current $\lambda_d$, see Figs. 1(b)–1(c).

Another typical piecewise linear representation for the diode characteristic is that shown in Fig. 2. The voltage–

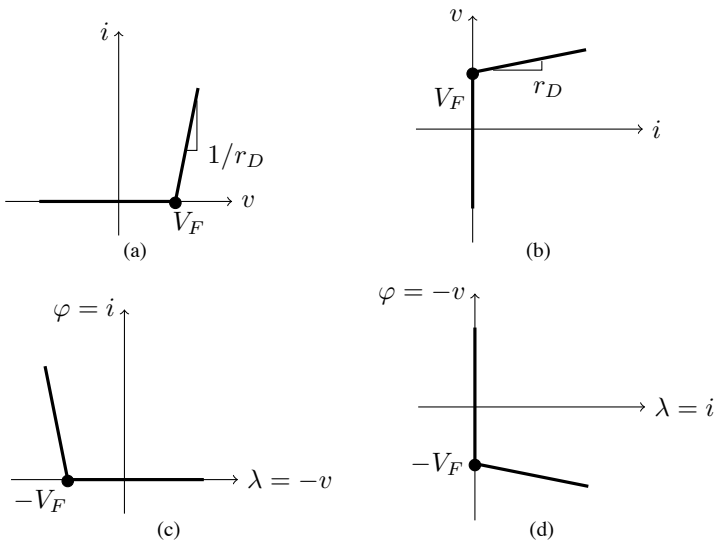


Fig. 2. Piecewise linear characteristics of a diode: (a) voltage–current characteristic, (b) current–voltage characteristic, (c) $(\varphi, \lambda)$ characteristic with input $\lambda = -v$ and output $\varphi = i$, (d) $(\varphi, \lambda)$ characteristic with input $\lambda = i$ and output $\varphi = -v$.

current characteristic in Fig. 2(c) can be represented by the following LC model:

$$\varphi = z_d \tag{5a}$$

$$w_d = \lambda + r_D z_d + V_F \tag{5b}$$

$$0 \leqslant w_d \perp z_d \geqslant 0 \tag{5c}$$

while the LC model of the current–voltage characteristic in Fig. 2(d) is given by

$$\varphi = z_d - V_F - r_D \lambda \tag{6a}$$

$$w_d = \lambda \tag{6b}$$

$$0 \leqslant w_d \perp z_d \geqslant 0. \tag{6c}$$

It is now possible to construct an LC model for an electronic switch characteristic, see Fig. 3. By considering a bipolar junction transistor the switch variables have the following meanings: $i_S$ is the collector current, $v_S$ is the collector-emitter voltage, $i_{\max}$ is the maximum collector current that the transistor can provide without damage, $\sigma \in [0, 1]$ is the normalized switch control signal proportional to the base current, – analogous interpretations of the physical meanings for $i_S$, $v_S$, $i_{\max}$ and $\sigma$ are possible for other electronic switches. Then for $\sigma = 0$ (OFF) the switching is blocking and the switch current $i_S$ is identically zero for any switch voltage $v_S$. For $\sigma = 1$ the switch is conducting (ON). The model also captures the switch operating condition in the so-called saturation region where the device can provide any current between 0 and $i_{\max}\sigma$.

Let us assume that the opposite of the diode voltage, say $\lambda_c = -v_S$ and the control signal $\sigma$ are given. Then the output variable of the switch model is chosen as the switch current $\varphi_c = i_S$. The subscript "c" is used to indicate

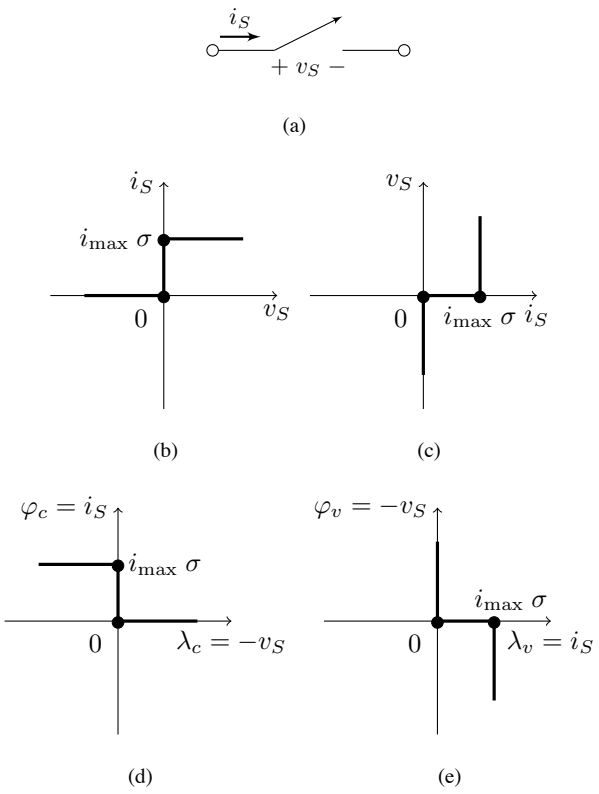


Fig. 3. Electronic switch: (a) symbol, (b) idealized voltage–current characteristic, (c) idealized current–voltage characteristic, (d) characteristic with $\lambda_c = -v_S$ and $\varphi_c = i_S$, (e) characteristic with $\lambda_v = i_S$ and $\varphi_v = -v_S$. Without loss of generality it is assumed that the switch is able to block also negative voltages.

that the variable $\varphi$ in this case is a current. Then the voltage–current characteristic in Fig. 3(d) can be represented with the following LC model

$$\varphi_c = z_{c_1} \tag{7a}$$

$$w_{c_1} = z_{c_2} + \lambda_c \tag{7b}$$

$$w_{c_2} = -z_{c_1} + i_{\max}\sigma \tag{7c}$$

$$0 \leqslant w_c \perp z_c \geqslant 0, \tag{7d}$$

where $w_c = \mathrm{col}(w_{c_1}, w_{c_2})$, $z_c = \mathrm{col}(z_{c_1}, z_{c_2})$, and $\mathrm{col}(\,\cdot\,)$ indicates a vector obtained by stacking in a unique column the column vectors in its argument. The model (7) is in the form (2)–(3) with $N = \begin{bmatrix} 1 & 0 \end{bmatrix}$, $q = \mathrm{col}(\lambda_c, i_{\max}\sigma)$ and

$$M = \begin{bmatrix} 0 & 1 \\ -1 & 0 \end{bmatrix}. \tag{8}$$

Expressions (7) can be explained by looking at the possible values assumed by $\lambda_c$. The following cases are possible,

see Fig. 3(d):

$$\lambda_c > 0 \Rightarrow w_{c_1} > 0 \Rightarrow z_{c_1} = 0 \Rightarrow \varphi_c = 0 \tag{9a}$$

$$\lambda_c < 0 \Rightarrow z_{c_2} > 0 \Rightarrow w_{c_2} = 0 \Rightarrow \varphi_c = z_{c_1} = i_{\max}\,\sigma \tag{9b}$$

$$\lambda_c = 0 \Rightarrow \{w_{c_1} \geqslant 0, z_{c_2} \geqslant 0\} \Rightarrow\ \varphi_c = z_{c_1} \in [0,\ i_{\max}\,\sigma]. \tag{9c}$$

For $\sigma \in [0, 1]$ the model (7) describes the set of possible voltage–current characteristics obtained by varying $\sigma$ between 0 and 1. The matrix (8) is positive semidefinite (and not P-matrix) and for $\lambda_c = 0$ the solution $z_c$ of (7) is not unique, see (9c). On the other hand among all possible solutions of (7), the following least-norm solution

$$\lambda_c > 0 \Rightarrow z_c = \mathrm{col}(0, 0) \tag{10a}$$

$$\lambda_c < 0 \Rightarrow z_c = \mathrm{col}(i_{\max}\sigma, -\lambda_c) \tag{10b}$$

$$\lambda_c = 0 \Rightarrow z_c = \mathrm{col}(0, 0) \tag{10c}$$

is unique.

An analysis similar to that presented above can be done if the switch current $i_S$ and the switch command $\sigma$ are given and the corresponding switch voltage must be found. Indeed one can consider the current–voltage characteristic shown in Fig. 3(e), where $\varphi_v = -v_S$ is the switch voltage and $\lambda_v = i_S$ is the switch current. A possible LC model can be written as

$$\varphi_v = z_{v_1} - z_{v_2} \tag{11a}$$

$$w_{v_1} = \lambda_v \tag{11b}$$

$$w_{v_2} = -\lambda_v + i_{\max}\sigma \tag{11c}$$

$$0 \leqslant w_v \perp z_v \geqslant 0, \tag{11d}$$

where $w_v = \mathrm{col}(w_{v_1}, w_{v_2})$ and $z_v = \mathrm{col}(z_{v_1}, z_{v_2})$. The model (11) is in the form (2)–(3) with $N = \begin{bmatrix} 1 & -1 \end{bmatrix}$, $q = \mathrm{col}(\lambda_v, -\lambda_v + i_{\max}\sigma)$ and $M$ being the zero matrix. The expressions (11) can be explained by considering the different ranges for $\lambda_v$. The following cases are possible

$$\lambda_v = 0 \Rightarrow \{w_{v_1} = 0, w_{v_2} = i_{\max}\,\sigma\} \Rightarrow \begin{cases} 0 < \sigma \leqslant 1 & \Rightarrow z_{v_2} = 0 \Rightarrow \varphi_v = z_{v_1} \geqslant 0 \\ \sigma = 0 & \Rightarrow \varphi_v = z_{v_1} - z_{v_2} \in \mathbb{R} \end{cases} \tag{12a}$$

$$\lambda_v = i_{\max}\sigma \Rightarrow \begin{cases} 0 < \sigma \leqslant 1 & \Rightarrow w_{v_1} > 0 \Rightarrow z_{v_1} = 0 \Rightarrow \varphi_v = -z_{v_2} \leqslant 0 \\ \sigma = 0 & \Rightarrow \text{see (12a)} \end{cases} \tag{12b}$$

$$0 < \lambda_v < i_{\max}\sigma \Rightarrow \{w_{v_1} > 0,\ w_{v_2} > 0\} \Rightarrow \varphi_v = 0. \tag{12c}$$

Consider also the antiparallel connection of an electronic switch and a diode. Assume that $\lambda$ is the opposite of the voltage across the parallel, that is equal to the voltage across the switch and $i$ is the total current through the parallel, that is the difference between the switch and the diode currents. By combining the voltage–current

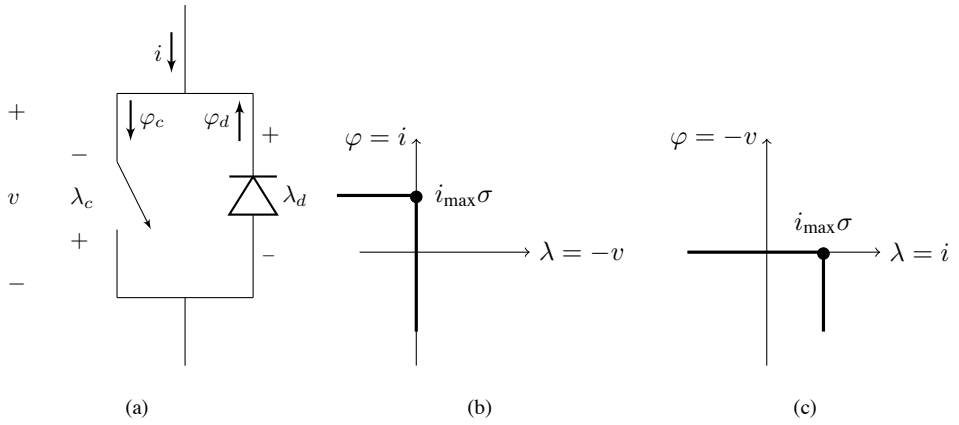


Fig. 4. Antiparallel connection of an electronic switch and a diode: (a) symbol, (b) idealized voltage-current characteristic, (c) idealized current-voltage characteristic.

characteristic $(\varphi_c, \lambda_c)$ of the electronic switch in Fig. 3(d) with the voltage–current characteristic $(\varphi_d, \lambda_d)$ of the diode in Fig. 1(d), one gets the voltage–current piecewise linear characteristic of the antiparallel connection in Fig. 4(b). The resulting characteristic has one breaking point and it can be modelled by the LC model

$$\varphi = -z + i_{\max}\sigma \tag{13a}$$

$$w = -\lambda \tag{13b}$$

$$0 \leqslant w \perp z \geqslant 0. \tag{13c}$$

The same reasoning can be repeated also when the voltage of the antiparallel connection is considered as the output and the current as the input, see Fig. 4(c). The corresponding LC model can be written as

$$\varphi = -z \tag{14a}$$

$$w = -\lambda + i_{\max}\sigma \tag{14b}$$

$$0 \leqslant w \perp z \geqslant 0. \tag{14c}$$

***Remark** 1:* The LC models of diodes and controlled switches are the basic elements from which more complex piecewise linear characteristics of electronic devices can be represented in the complementarity form. For the sake of simplicity in the sequel only the LC models (4), (7) and (11) will be considered, though the modeling approach proposed in this paper can be extended to the case of more involved piecewise linear characteristics of electronic devices.

The LC models of the electronic devices can be suitably collected into a compact complementarity representation which is useful for the formulation of the entire power converter complementarity model. Let us assume that the power converter under investigation has $N_d$ diodes, $N_c$ switches with currents as output variables and $N_v$ switches with voltages as output variables. With some abuse of notation let us redefine the following variables: $\varphi_d$ and $\lambda_d$ are the column vectors whose components are the voltages and currents through the $N_d$ diodes, $\varphi_c$ is the column vector

of the $N_c$ switches currents and $\lambda_c$ are the corresponding voltages, $\varphi_v$ is the column vector of the $N_v$ switches voltages and $\lambda_v$ are the corresponding currents.

By defining the column vectors

$$\varphi = \mathrm{col}(\varphi_d, \varphi_c, \varphi_v), \tag{15a}$$

$$\lambda = \mathrm{col}(\lambda_d, \lambda_c, \lambda_v), \tag{15b}$$

$$w_o = \mathrm{col}(w_d, w_c, w_v), \tag{15c}$$

$$z_o = \mathrm{col}(z_d, z_c, z_v), \tag{15d}$$

$$\sigma = \mathrm{col}(\sigma_c, \sigma_v), \tag{15e}$$

the LC model obtained by collecting all devices characteristics can be written as

$$\varphi = B_\varphi z_o \tag{16a}$$

$$w_o = C_\varphi \lambda + D_\varphi z_o + G_\varphi \sigma \tag{16b}$$

$$0 \leqslant w_o \perp z_o \geqslant 0, \tag{16c}$$

where $B_\varphi$, $C_\varphi$, $D_\varphi$ and $G_\varphi$ can be easily obtained.

The model (16) is in the form (2)–(3) with $N = B_\varphi$, $q = C_\varphi \lambda + G_\varphi \sigma$ and $M = D_\varphi$. Then the idealized characteristic of electronic devices commonly present in a generic power converter can be represented in the compact LC form (16).

## III. Complementarity dynamic model

In this section it is shown that the model of a wide class of *closed-loop* power converters can be written in the following dynamic LC form

$$\dot{x} = Ax + Bz + Ee \tag{17a}$$

$$w = Cx + Dz + Fe \tag{17b}$$

$$0 \leqslant w \perp z \geqslant 0, \tag{17c}$$

where $x$ is the state vector, $w$ and $z$ are complementarity variables, $e$ is the vector of the exogenous inputs and $A$, $B$, $C$, $D$, $E$, $F$ are *constant* matrices of suitable dimensions.

The construction of the complementarity model is modular in the sense that it directly follows by associating the converter dynamic model – derived by standard methods and depending only on its topology – with the electronic devices characteristics. A block scheme representation, corresponding to the model (17) decomposed into its major subsystems, is shown in Fig. 5. The model construction procedure is applied step-by-step to a boost DC–DC converter with voltage-mode pulse-width modulation (PWM) control, see Fig.s 6 and 7.

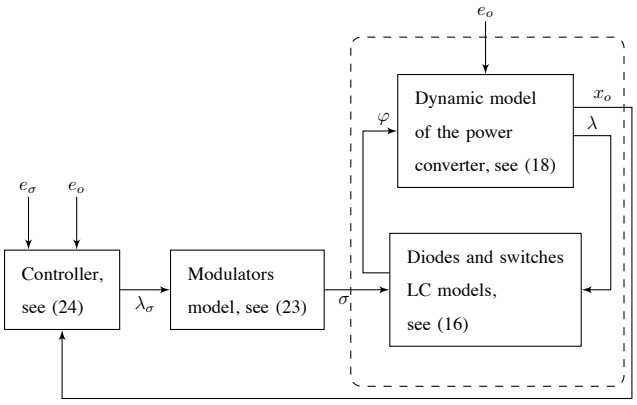


Fig. 5. Block diagram of the LC model for a closed-loop power converter.

### *A. Open-loop LC model*

As a preliminary step it is shown that a dynamic model of *open-loop* power converters can be written in the form (17). A typical approach for deriving a power converter dynamical model consists of extracting the diodes and switches to the ports and applying the Kirchhoff laws to the branches (and links) of a proper tree of the graph associated to the circuit, [32]. In particular, suppose that the capacitors do not form a loop (with or without voltage sources) and inductors do not form a cut set (with or without current sources). Then by applying the Kirchhoff laws, a state-space model in the following form can be obtained

$$\dot{x}_o = A_o x_o + B_o \varphi + E_o e_o \tag{18a}$$

$$\lambda = C_o x_o + D_o \varphi + F_o e_o, \tag{18b}$$

where $x_o \in \mathbb{R}^{N_o}$ is the state vector of the open-loop system, $e_o$ denotes the vector of the external sources for the open-loop system and $(\varphi, \lambda)$ are the voltage–current or current–voltage pairs of the electronic devices.

By using (16) with (18) the model of an open-loop power converter can be written in the following LC form

$$\dot{x}_o = A_o x_o + B_o B_\varphi z_o + E_o e_o \tag{19a}$$

$$w_o = C_\varphi C_o x_o + (C_\varphi D_o B_\varphi + D_\varphi) z_o + C_\varphi F_o e_o + G_\varphi \sigma \tag{19b}$$

$$0 \leqslant w_o \perp z_o \geqslant 0. \tag{19c}$$

The model (19) corresponds to the dashed boxed block in Fig. 5, with $w_o$ and $z_o$ being 'internal' complementarity variables, $x_o$ the state vector, $e_o$ the exogenous input and $\sigma$ the control input, i.e., the vector of the commands to the electronic switches. For open-loop controlled converters the vector $\sigma$ can be included into the exogenous vector $e_o$, then the model (19) is in the form (17).

As an illustrative example consider the boost DC–DC converter depicted in Fig. 6. Denote $e_o$ the input voltage, $x_{o_1}$ the inductor current, $x_{o_2}$ the capacitor voltage, $(\varphi_c, \lambda_c)$ the current–voltage pair of the electronic switch, $(\varphi_d, \lambda_d)$

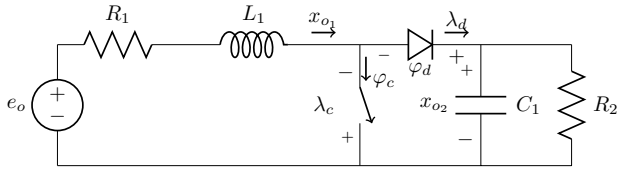


Fig. 6. Boost DC–DC converter.

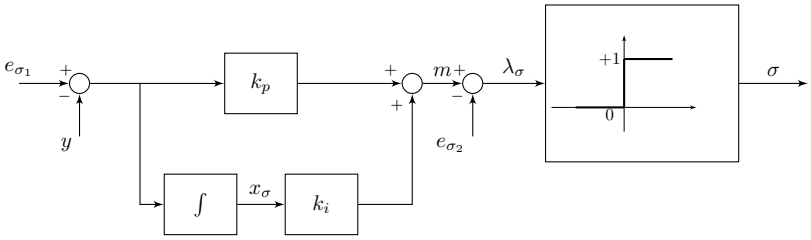


Fig. 7. Block diagram of a proportional–integral controller: $e_{\sigma_1}$ is the reference signal for the output variable $y$; $m$ is the modulation signal; $e_{\sigma_2}$ is the carrier signal; $x_\sigma$ is the controller state variable (the integral of the error); $k_p$ and $k_i$ are the proportional and integral gains, respectively; $\sigma$ is the switching signal.

the voltage–current pair of the diode. By applying the Kirchhoff laws, the circuit model can be written as follows

$$\dot{x}_{o_1} = -\frac{R_1}{L_1}x_{o_1} - \frac{1}{L_1}x_{o_2} + \frac{1}{L_1}\varphi_d + \frac{1}{L_1}e_o \tag{20a}$$

$$\dot{x}_{o_2} = \frac{1}{C_1}x_{o_1} - \frac{1}{R_2C_1}x_{o_2} - \frac{1}{C_1}\varphi_c \tag{20b}$$

$$\lambda_d = x_{o_1} - \varphi_c \tag{20c}$$

$$\lambda_c = -x_{o_2} + \varphi_d \tag{20d}$$

which is in the form (18) with $x_o = \mathrm{col}(x_{o_1}, x_{o_2})$, $\varphi = \mathrm{col}(\varphi_d, \varphi_c)$ and $\lambda = \mathrm{col}(\lambda_d, \lambda_c)$.

By using (4) and (7), or equivalently by considering (16) with $N_d = N_c = 1$ and $N_v = 0$, the devices characteristics can be represented as follows

$$\varphi_d = z_d \tag{21a}$$

$$\varphi_c = z_{c_1} \tag{21b}$$

$$w_d = \lambda_d \tag{21c}$$

$$w_{c_1} = \lambda_c + z_{c_2} \tag{21d}$$

$$w_{c_2} = -z_{c_1} + i_{\max}\sigma \tag{21e}$$

$$0 \leqslant w_o \perp z_o \geqslant 0 \tag{21f}$$

which are in the form (16) with $\varphi = \mathrm{col}(\varphi_d, \varphi_c)$, $\lambda = \mathrm{col}(\lambda_d, \lambda_c)$, $z_o = \mathrm{col}(z_d, z_{c_1}, z_{c_2})$ and $w_o = \mathrm{col}(w_d, w_{c_1}, w_{c_2})$. Then by combining (20) and (21) the open-loop LC model takes the form (17) with $e = \mathrm{col}(e_o, \sigma)$.

*B. Closed-loop LC model*

The *closed-loop* LC model of power converters can be obtained by specifying the dependencies of the $N_s = N_c + N_v$ switching signals $\sigma$ on the state and on the exogenous inputs. As an example consider that the switches are controlled by means of a PWM technique. Then define $\lambda_\sigma$ as the difference between the modulation signal $m$ and the carrier signal $e_{\sigma_2}$, and $\sigma$ as a step function whose argument is $\lambda_\sigma$, see Fig. 7. A scalar switching signal $\sigma$ can be represented by means of the following LC model

$$\sigma = z_{\sigma_1} \tag{22a}$$

$$w_{\sigma_1} = z_{\sigma_2} - \lambda_\sigma \tag{22b}$$

$$w_{\sigma_2} = -z_{\sigma_1} + 1 \tag{22c}$$

$$0 \leqslant w_\sigma \perp z_\sigma \geqslant 0, \tag{22d}$$

where $w_\sigma = \mathrm{col}(w_{\sigma_1}, w_{\sigma_2})$, $z_\sigma = \mathrm{col}(z_{\sigma_1}, z_{\sigma_2})$. The model (22) can be explained by considering the sign of $\lambda_\sigma$. If $\lambda_\sigma < 0$, since $z_{\sigma_2}$ is nonnegative, from (22b) it will be $w_{\sigma_1}$ strictly positive and, by the using complementarity constraint (22d), from (22a) we get $\sigma = z_{\sigma_1} = 0$, i.e., the switch is OFF. If $\lambda_\sigma > 0$ from (22b) it must be $z_{\sigma_2}$ strictly positive and then, by using the complementarity constraint (22d), it will be $w_{\sigma_2} = 0$, and (22c) with (22a) leads to $\sigma = z_{\sigma_1} = 1$, i.e., the switch is ON. Finally, if $\lambda_\sigma = 0$ the equation (22b) does not impose any constraint on $z_{\sigma_2}$ and then (22b) with the nonnegative constraint on $w_{\sigma_1}$ implies that $\sigma = z_{\sigma_1}$ can take any value within the interval $[0, 1]$.

By using (22), the $N_s$ switching signals can be represented all together in the following compact complementarity form

$$\sigma = B_\sigma z_\sigma \tag{23a}$$

$$w_\sigma = C_\sigma \lambda_\sigma + D_\sigma z_\sigma + \gamma_\sigma \tag{23b}$$

$$0 \leq w_\sigma \perp z_\sigma \geq 0, \tag{23c}$$

where $z_\sigma \in \mathbb{R}^{2N_s}$ is the vector of all complementarity variables required to represent the switching signals, and the matrices can be simply obtained.

In order to complete the closed-loop LC model of a power converter, a model of the controller must be constructed, see Fig. 5. In particular, for a wide class of practical controllers the control signal can be represented as the output of a linear dynamic model that computes its control action by using information on the power converter state $x_o$ and, possibly, on other exogenous signals

$$\dot{x}_\sigma = A_\sigma x_\sigma + A_{\sigma o} x_o + E_{\sigma o} e_o + E_{\sigma e} e_\sigma \tag{24a}$$

$$\lambda_\sigma = C_{m\sigma} x_\sigma + C_{mo} x_o + F_{me} e_\sigma \tag{24b}$$

with $x_\sigma \in \mathbb{R}^{N_\sigma}$ being the state of the controller and $e_\sigma$ having the reference inputs and other control inputs as components.

***Remark** 2:* The complementarity framework can be used to represent a more general class of controllers, e.g., those consisting of linear parts combined with piecewise linear, quantized or hysteretic characteristics, or more in general all relationships representable within the complementarity framework. In these cases LC models of piecewise linear characteristics and algebraic manipulations, similar to those presented in this paper, allow to write the closed-loop power converter in the form (17). In Section VI-C this will be demonstrated for current-mode controlled power converters.

The complementarity model corresponding to the block scheme in Fig. 5 is then complete. In particular: (24) is the controller model, (23) is the modulator model and (19) is the model of the circuit including the electronic devices characteristics (the dash boxed block). By collecting (19)–(24) and by defining

$$x = \mathrm{col}(x_o, x_\sigma), \tag{25a}$$

$$e = \mathrm{col}(e_o, e_\sigma, 1_{N_s}), \tag{25b}$$

$$z = \mathrm{col}(z_o, z_\sigma), \tag{25c}$$

$$w = \mathrm{col}(w_o, w_\sigma), \tag{25d}$$

the complete model of the controlled power converter can be written in the form (17) with

$$A = \begin{bmatrix} A_o & 0 \\ A_{\sigma o} & A_\sigma \end{bmatrix}, \tag{26a}$$

$$B = \begin{bmatrix} B_o B_\varphi & 0 \\ 0 & 0 \end{bmatrix}, \tag{26b}$$

$$C = \begin{bmatrix} C_\varphi C_o & 0 \\ C_\sigma C_{mo} & C_\sigma C_{m\sigma} \end{bmatrix}, \tag{26c}$$

$$D = \begin{bmatrix} C_\varphi D_o B_\varphi + D_\varphi & G_\varphi B_\sigma \\ 0 & D_\sigma \end{bmatrix}, \tag{26d}$$

$$E = \begin{bmatrix} E_o & 0 & 0 \\ E_{\sigma o} & E_{\sigma e} & 0 \end{bmatrix}, \tag{26e}$$

$$F = \begin{bmatrix} C_\varphi F_o & 0 & 0 \\ 0 & C_\sigma F_{me} & \gamma_\sigma \end{bmatrix}. \tag{26f}$$

It is important to highlight that the model (17) contains all the possible operating modes of the closed-loop power converter and that the matrices $A$, $B$, $C$, $D$, $E$, $F$ are constant.

Going back to the boost illustrative example, consider a proportional–integral controller whose input is the error between the output voltage $y = x_{o_2}$ and its reference value, say $e_{\sigma_1}$, see Fig. 7. By indicating with $x_\sigma$ the state variable corresponding to the output of the integrator, with $e_{\sigma_2}$ the carrier signal, with $k_p$ and $k_i$ the proportional

and integral gains of the controller, respectively, the controller dynamics can be written as

$$\dot{x}_\sigma = -x_{o_2} + e_{\sigma_1} \tag{27a}$$

$$\lambda_\sigma = k_i\, x_\sigma - k_p\, x_{o_2} + k_p\, e_{\sigma_1} - e_{\sigma_2} \tag{27b}$$

which are in the form (24) with $e_\sigma = \mathrm{col}(e_{\sigma_1}, e_{\sigma_2})$.

The switching signal $\sigma$ can be expressed by using the model (22). Let us define $x = \mathrm{col}(x_o, x_\sigma)$, $e = \mathrm{col}(e_o, e_\sigma)$. By using (26), or equivalently by substituting (22a) in (21e) and (27b) in (22b), the closed-loop model can be written in the dynamic LC form (17) with the following matrices

$$A = \begin{bmatrix} -\frac{R_1}{L_1} & -\frac{1}{L_1} & 0 \\ \frac{1}{C_1} & -\frac{1}{R_2 C_1} & 0 \\ 0 & -1 & 0 \end{bmatrix}, \tag{28a}$$

$$B = \begin{bmatrix} \frac{1}{L_1} & 0 & 0 & 0 & 0 \\ 0 & -\frac{1}{C_1} & 0 & 0 & 0 \\ 0 & 0 & 0 & 0 & 0 \end{bmatrix}, \tag{28b}$$

$$C = \begin{bmatrix} 1 & 0 & 0 \\ 0 & -1 & 0 \\ 0 & 0 & 0 \\ 0 & k_p & -k_i \\ 0 & 0 & 0 \end{bmatrix}, \tag{28c}$$

$$D = \begin{bmatrix} 0 & -1 & 0 & 0 & 0 \\ 1 & 0 & 1 & 0 & 0 \\ 0 & -1 & 0 & i_{\max} & 0 \\ 0 & 0 & 0 & 0 & 1 \\ 0 & 0 & 0 & -1 & 0 \end{bmatrix}, \tag{28d}$$

$$E = \begin{bmatrix} \frac{1}{L_1} & 0 & 0 & 0 \\ 0 & 0 & 0 & 0 \\ 0 & 1 & 0 & 0 \end{bmatrix}, \tag{28e}$$

$$F = \begin{bmatrix} 0 & 0 & 0 & 0 \\ 0 & 0 & 0 & 0 \\ 0 & 0 & 0 & 0 \\ 0 & -k_p & 1 & 0 \\ 0 & 0 & 0 & 1 \end{bmatrix}. \tag{28f}$$

The LC model (17) with the matrices (28) represents the dynamic evolutions of the closed-loop DC-DC boost converter for all possible operating modes, initial conditions and exogenous inputs.

## IV. TIME-STEPPING AND STEADY-STATE SOLUTIONS

The model (17) can be used to compute the transient time-stepping evolution and the steady-state oscillation exhibited by a controlled converter. To this aim let us discretize the system (17) with a sampling period $h$. By considering, for instance, the Tustin method one obtains the following discrete-time system

$$x_k - A_z x_{k-1} = B_z(z_{k-1} + z_k) + E_z(e_{k-1} + e_k) \tag{29a}$$

$$w_k = Cx_k + Dz_k + Fe_k \tag{29b}$$

$$0 \leqslant w_k \perp z_k \geqslant 0 \tag{29c}$$

with $k = 1, 2, \ldots, N_h$, $x_k = x(kh)$ and analogously for the other variables, and the matrices are given by

$$A_z = \left(I_{N_x} - \frac{h}{2}A\right)^{-1}\left(I_{N_x} + \frac{h}{2}A\right), \tag{30a}$$

$$B_z = \frac{h}{2}\left(I_{N_x} - \frac{h}{2}A\right)^{-1}B, \tag{30b}$$

$$E_z = \frac{h}{2}\left(I_{N_x} - \frac{h}{2}A\right)^{-1}E, \tag{30c}$$

where $I_{N_x}$ is the $N_x \times N_x$ identity matrix and $N_x = N_o + N_\sigma$ is the number of the state variables of the closed-loop power converter.

Given $z_{k-1}$, $e_{k-1}$, $e_k$ and $x_{k-1}$, one can solve (29a) for $x_k$ and substitute this value in (29b) that, together with (29c), will be used for finding $z_k$. Therefore the time-stepping evolution can be obtained by iterating the solution of LC problems in the form

$$w_k = Mz_k + q_k \tag{31a}$$

$$0 \leqslant w_k \perp z_k \geqslant 0 \tag{31b}$$

with

$$M = CB_z + D \tag{32}$$

and

$$q_k = CA_z x_{k-1} + (CE_z + F)e_k + CB_z z_{k-1} + CE_z e_{k-1} \tag{33}$$

for $k = 1, 2, \ldots, N_h$. Each LC problem (31) can be solved by using standard (and efficient) algorithms widely studied in the complementarity literature [7].

The dynamic LC model (29) can be used also to compute steady-state oscillations exhibited by closed-loop power converters. Let us assume that the system (17) has a periodic absolutely continuous solution $x(t) = x(t + T)$ for every continuous-time instant $t$ with $T$ being the known period of the solution. We assume that the convergence property holds, i.e., the continuous piecewise linear interpolation of the samples sequence $x_k$ given by (29) converges to the continuous-time solution $x(t)$ of (17) as $h = T/N_h$ goes to zero. In particular, we assume that (29) has a periodic solution of period $N_h$, approximating the periodic continuous-time solution of period $T$ of the system (17).

By defining

$$\bar{x} = \text{col}(x_1,\ x_2, \ldots,\ x_{N_h}), \tag{34a}$$

$$\bar{e} = \text{col}(e_1,\ e_2, \ldots,\ e_{N_h}), \tag{34b}$$

$$\bar{z} = \text{col}(z_1,\ z_2, \ldots,\ z_{N_h}), \tag{34c}$$

$$\bar{w} = \text{col}(w_1,\ w_2, \ldots,\ w_{N_h}) \tag{34d}$$

with $\overline{x} \in \mathbb{R}^{N_x \cdot N_h}$, $\overline{z} \in \mathbb{R}^{(4N_s+N_d) \cdot N_h}$ and by using the periodicity condition $x_0 = x_{N_h}$, we can write simultaneously the equations (29) along the period $N_h$ which leads to

$$0 = \overline{A}\overline{x} + \overline{B}\overline{z} + \overline{E}\,\overline{e} \tag{35a}$$

$$\overline{w} = \overline{C}\overline{x} + \overline{D}\overline{z} + \overline{F}\,\overline{e} \tag{35b}$$

with

$$\overline{A} = \begin{bmatrix} -I_{N_x} & 0 & \cdots & 0 & A_z \\ A_z & -I_{N_x} & \cdots & 0 & 0 \\ \vdots & \vdots & \ddots & \vdots & \vdots \\ 0 & 0 & \cdots & A_z & -I_{N_x} \end{bmatrix}, \tag{36a}$$

$$\overline{B} = \begin{bmatrix} B_z & 0 & \cdots & 0 & B_z \\ B_z & B_z & \cdots & 0 & 0 \\ \vdots & \vdots & \ddots & \vdots & \vdots \\ 0 & 0 & \cdots & B_z & B_z \end{bmatrix}, \tag{36b}$$

$$\overline{C} = I_{N_h} \otimes C, \tag{36c}$$

$$\overline{D} = I_{N_h} \otimes D, \tag{36d}$$

$$\overline{E} = \begin{bmatrix} E_z & 0 & \cdots & 0 & E_z \\ E_z & E_z & \cdots & 0 & 0 \\ \vdots & \vdots & \ddots & \vdots & \vdots \\ 0 & 0 & \cdots & E_z & E_z \end{bmatrix}, \tag{36e}$$

$$\overline{F} = I_{N_h} \otimes F, \tag{36f}$$

where $\otimes$ denotes the Kronecker product.

***Remark** 3:* By discretizing (17) with the backward Euler or the Zero–Order–Hold techniques and by using similar arguments, one can obtain corresponding representations in the form (35) with suitable $\overline{A}$, $\overline{B}$, $\overline{C}$, $\overline{D}$, $\overline{E}$, $\overline{F}$.

From (36a) one obtains

$$\det(\overline{A}) = (-1)^{N_h} \det(I_{N_x} - A_z^{N_h}) \tag{37}$$

then $\overline{A}$ is invertible if $A_z$ has no eigenvalues in 1, which corresponds to $A$ having no eigenvalues in the origin, see (30a).

If the matrix $\overline{A}$ is invertible, the periodic solution of (29) can be obtained by formulating a suitable LC problem. Indeed by solving (35a) for the vector $\overline{x}$ we obtain

$$\overline{x} = -\overline{A}^{-1}(\overline{B}\,\overline{z} + \overline{E}\,\overline{e}). \tag{38}$$

Then by substituting (38) in (35b) we obtain

$$\overline{w} = M\overline{z} + q \tag{39a}$$

$$0 \leqslant \overline{w} \perp \overline{z} \geqslant 0 \tag{39b}$$

with

$$M = -\overline{CA}^{-1}\overline{B} + \overline{D} \tag{40}$$

and

$$q = (-\overline{CA}^{-1}\overline{E} + \overline{F})\,\overline{e}, \tag{41}$$

which is a classical LC problem in the form (2). The solution $\overline{z}$ can be used in (38) to obtain the periodic steady-state solution $\overline{x}$.

***Remark 4:*** If the matrix $\overline{A}$ is not invertible (which is the case for the closed-loop boost converter considered above, see (28a), (30a) and (37)), one can define a mixed LC problem (1) which allows to avoid the inversion of $\overline{A}$ for the computation of the periodic solution. Indeed the system (35) can be written in the form (1) by defining

$$z = \text{col}(\overline{x}, \overline{z}), \tag{42a}$$

$$M = \begin{bmatrix} \overline{A} & \overline{B} \\ \overline{C} & \overline{D} \end{bmatrix}, \tag{42b}$$

$$q = \begin{bmatrix} \overline{E} \\ \overline{F} \end{bmatrix} \overline{e}, \tag{42c}$$

$$l = \text{col}(-\infty_{N_x \cdot N_h}, 0), \tag{42d}$$

$$u = \text{col}(+\infty_{N_x \cdot N_h}, +\infty_{(4N_s+N_d) \cdot N_h}), \tag{42e}$$

where $\infty_N$ is the $N$-th dimensional vector of $\infty$. The choice of infinite lower and upper bounds implies that the variable $w$ and the variable $v$ associated to $\overline{x}$ are zero. This permits to formulate (35) as a mixed LC problem.

## V. Open-loop power converters analysis

The approach for the computation of the steady-state solution can be used to determine the control-to-output frequency response of power converters, that is usually calculated by considering open-loop models. Then in the following, we refer to the application of the technique presented in the previous section by considering the matrices

$$A = A_o,\ B = B_o B_\varphi,\ C = C_\varphi C_o,\ D = C_\varphi D_o B_\varphi + D_\varphi, \tag{43}$$

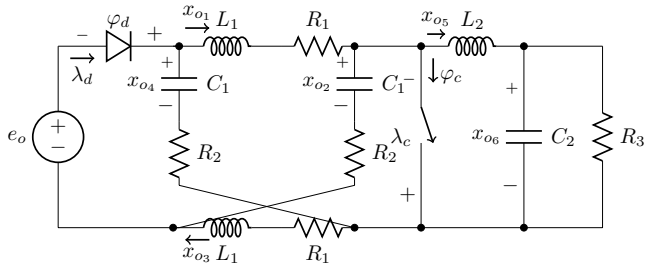


Fig. 8. Z-source DC–DC power converter.

see (17) and (19). A useful property for such analysis is the uniqueness of the steady-state solution $\overline{x}$ which corresponds to the unique least-norm solution $\overline{z}$ of the LC problem (39)–(41), or if $\overline{A}$ is not invertible to the solution of the mixed LC problem (1) with (42). Conditions for such uniqueness can be obtained by using the passivity concept. In particular, if the open-loop model (18) of a power converter is passive with respect to the input $\varphi$ and the output $\lambda$ (with $\varphi$ and $\lambda$ being the input-output of the discussed idealized electronic devices), then the complementarity problem (39) has a unique least-norm solution.

As an example let us consider the Z-source DC–DC converter in Fig. 8 where $e_o$ is the input voltage, $x_{o_1},\ x_{o_3},\ x_{o_5}$ are the currents of the inductors, $x_{o_2},\ x_{o_4},\ x_{o_6}$ are the voltages of the capacitors, $(\varphi_c, \lambda_c)$ is the current–voltage pair of the electronic switch, $(\varphi_d, \lambda_d)$ is the voltage–current pair of the diode. By applying the Kirchhoff laws to the circuit one obtains

$$\dot{x}_{o_1} = -\frac{(R_1+R_2)}{L_1}x_{o_1} - \frac{1}{L_1}x_{o_2} + \frac{R_2}{L_1}x_{o_5} + \frac{1}{L_1}\varphi_d + \frac{R_2}{L_1}\varphi_c + \frac{1}{L_1}e_o \tag{44a}$$

$$\dot{x}_{o_2} = \frac{1}{C_1}x_{o_1} - \frac{1}{C_1}x_{o_5} - \frac{1}{C_1}\varphi_c \tag{44b}$$

$$\dot{x}_{o_3} = -\frac{(R_1+R_2)}{L_1}x_{o_3} - \frac{1}{L_1}x_{o_4} + \frac{R_2}{L_1}x_{o_5} + \frac{1}{L_1}\varphi_d + \frac{R_2}{L_1}\varphi_c + \frac{1}{L_1}e_o \tag{44c}$$

$$\dot{x}_{o_4} = \frac{1}{C_1}x_{o_3} - \frac{1}{C_1}x_{o_5} - \frac{1}{C_1}\varphi_c \tag{44d}$$

$$\dot{x}_{o_5} = \frac{R_2}{L_2}x_{o_1} + \frac{1}{L_2}x_{o_2} + \frac{R_2}{L_2}x_{o_3} + \frac{1}{L_2}x_{o_4} - 2\frac{R_2}{L_2}x_{o_5} - \frac{1}{L_2}x_{o_6} - \frac{1}{L_2}\varphi_d - 2\frac{R_2}{L_2}\varphi_c - \frac{1}{L_2}e_o \tag{44e}$$

$$\dot{x}_{o_6} = \frac{1}{C_2}x_{o_5} - \frac{1}{R_3C_2}x_{o_6} \tag{44f}$$

$$\lambda_d = x_{o_1} + x_{o_3} - x_{o_5} - \varphi_c \tag{44g}$$

$$\lambda_c = -R_2x_{o_1} - x_{o_2} - R_2x_{o_3} - x_{o_4} + 2R_2x_{o_5} + \varphi_d + 2R_2\varphi_c + e_o \tag{44h}$$

which is the model in the form (18) with $x_o = \mathrm{col}(x_{o_1}, x_{o_2}, x_{o_3}, x_{o_4}, x_{o_5}, x_{o_6})$, $\varphi = \mathrm{col}(\varphi_d, \varphi_c)$ and $\lambda = \mathrm{col}(\lambda_d, \lambda_c)$. It is easy to show that the model is passive with respect to the input $\varphi$ and the output $\lambda$.

Moreover by substituting the switch and the diode complementarity models (7) and (4), respectively, the resulting Z-source converter model in the form (19) is passive with respect to the input $z_o$ and the output $w_o$.

A typical approach in order to obtain the control-to-output frequency response of power converters consists of

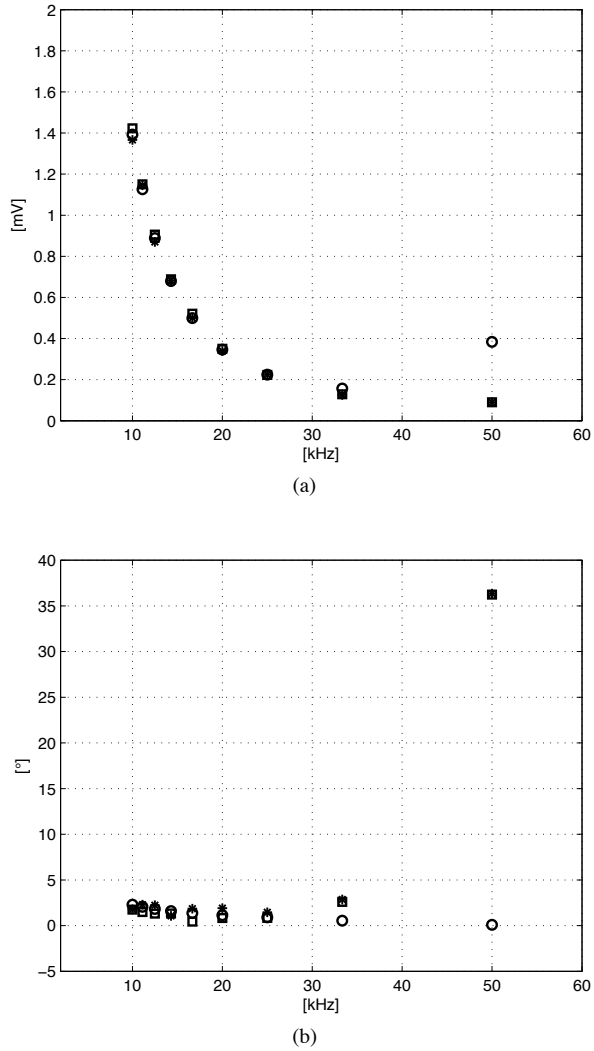


Fig. 9. First harmonics of the output voltage of the Z-source converter obtained with the LC steady-state approach (*), the averaged model (o) and the analytical solution (□) for different values of $N_p$.

considering a PWM with sinusoidal modulation signal $e_{\sigma_1} = V_0 + V_1 \sin(2\pi t/T)$ and a periodic carrier signal, say $e_{\sigma_2}$. Without loss of generality it is useful to consider the modulation signal period $T$ proportional to the carrier signal period $T_c$, i.e., $T = N_p T_c$ where $N_p$ is a positive integer. The sampling period $h$ can be chosen as $h = T/N_h = T_c N_p / N_h$. By considering Fig. 7 without the feedback, i.e., $y = 0$, $k_p = 1$ and $k_i = 0$, one can write

$$\lambda_\sigma = e_{\sigma_1} - e_{\sigma_2}, \tag{45}$$

which is in the form (24b). The model of the power converter can be written in the form (17) by using (44) with (4) for the pair $(\varphi_d, \lambda_d)$, (7) for the pair $(\varphi_c, \lambda_c)$, (22) for the switching signal $\sigma$, (45) for the variable $\lambda_\sigma$ and by defining $x = x_o$, $e = \mathrm{col}(e_o, e_{\sigma_1}, e_{\sigma_2}, 1)$, $z = \mathrm{col}(z_d, z_{c_1}, z_{c_2}, z_{\sigma_1}, z_{\sigma_2})$ and $w = \mathrm{col}(w_d, w_{c_1}, w_{c_2}, w_{\sigma_1}, w_{\sigma_2})$.

The proposed LC approach for the computation of the steady-state solution can be applied to the resulting model.

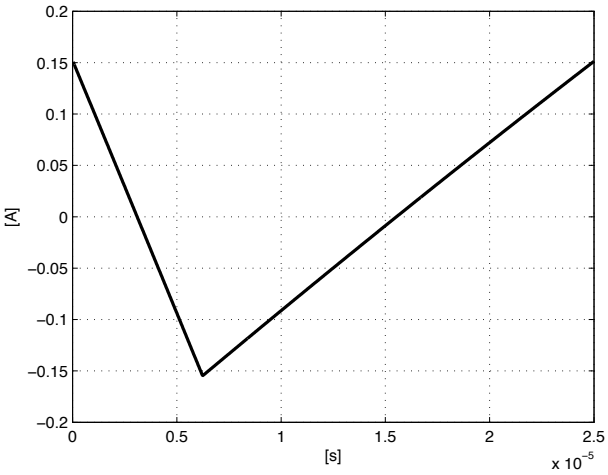


Fig. 10. Current through the filter capacitor $C_2$.

Consider the following circuit parameters $L_1 = 175$ μH, $C_1 = 220$ μF, $R_1 = 0.42\ \Omega$, $R_2 = 0.22\ \Omega$, $R_3 = 50\ \Omega$, $L_2 = 330$ μH, $C_2 = 470$ μF, and $i_{\max} = 5$ A and $e_o = 12$ V. The modulation voltage $e_{\sigma 1}$ is a sinusoidal signal with $V_0 = 0.3$ V and $V_1 = 0.03$ V and the carrier signal $e_{\sigma 2}$ is a sawtooth with unitary amplitude and frequency $1/T_c = 100$ kHz. Figure 9 shows the amplitude and the phase of the first harmonic of the steady-state output voltage $x_{o_6}$ obtained by varying $N_p = 2, 3, \ldots, 10$ with $N_h = 4000$, compared with the results obtained by using the averaged model and the analytical solution obtained by considering the a priori knowledge of the commutation time instants and the sequence of the modes. These data are not required for the computation of the complementarity solution which provides these information as results.

Figure 9 confirms the good accuracy of the complementarity approach whose results are very close to the analytical solution. Instead, at 50 kHz, corresponding to $N_p = 2$, we can note the accuracy reduction of the averaged model when the frequencies of the modulation and carrier signals become closer.

The LC model captures the switched behavior of the converter independently of the modulation frequency, provided that a sufficiently small sampling period $h$ is selected.

Once again it is important to highlight that the same LC model is valid for all operating conditions and does not require the a priori knowledge of the modes sequence.

In the following, the control-to-output response is obtained by considering a constant control voltage, as in [33] where a Z-source converter with the parasitic resistances is considered. The model of the Z-source converter is built by considering the complementarity model of the diode and the electronic switch with parasitics, see Section II. In order to prove the efficiency of the proposed approach, we have compared our results with the theoretical and experimental results presented in [33], see Fig. 10 and Table I. In particular, Fig. 10 shows the steady-state evolution of the current through the filter capacitor $C_2$, while Table I summarizes the values of some key parameters corresponding to the steady-state analysis. The validity of the complementarity approach is confirmed.

| Parameter | Predicted Value [33] | Measured Value [33] | MLCP procedure |
|---|---|---|---|
| average $x_{o_2}$ | 16.34 V | 16.2 V | 16.33 V |
| inductor $L_1$ voltage (switch ON) | 16.34 V | 16 V | 16.33 V |
| inductor $L_1$ voltage (switch OFF) | $-4.34$ V | $-4.6$ V | $-4.33$ V |
| inductor $L_f$ voltage (switch ON) | $-16.34$ V | $-16$ V | $-16.13$ V |
| inductor $L_f$ voltage (switch OFF) | $-4.34$ V | $-4.6$ V | $-4.13$ V |
| peak-to-peak inductor $L_1$ current | 309.5 mA | 310 mA | 309.27 mA |
| peak-to-peak inductor $L_f$ current | 309.5 mA | 312.5 mA | 306.13 mA |

TABLE I

THEORETICAL, EXPERIMENTAL AND SIMULATION RESULTS

## VI. SOME EXAMPLES OF CLOSED-LOOP POWER CONVERTERS ANALYSIS

The proposed LC modeling approach can be used for the computation of the transient and steady-state solutions of closed-loop power converters. Before analyzing some examples, it is interesting to make a preliminar consideration on the passivity of closed-loop power converters. We were not able to find a power converter with a closed-loop model being passive with respect to the complementarity variables: for all cases analyzed the passivity property is lost when going from open-loop to closed-loop models. If the closed-loop complementarity model is not passive, it is not possible to conclude the uniqueness of the solution of (39). However, the interesting thing is that closed-loop converters can be still analyzed by using the complementarity modeling approach and the steady-state computation procedure presented above. Indeed, for determining the multiple solutions one can enlarge the complementarity problem with opportune constraints [34] or initialize the LC problem solver with different initial guesses [30].

The numerical results, presented in this section, are verified by considering the corresponding results provided by PLECS, a toolbox for Simulink/MATLAB that is specifically designed for the simulation and analysis of power electronics systems [35]. In particular the PLECS steady-state results are obtained by using the Steady-State Analysis Block and the continuous-time state-space method which requires to use the variable-step Simulink solver. All LC problems are solved by using the PATH tool [30].

### *A. Boost converter in discontinuous conduction mode*

Consider the boost DC–DC converter shown in Fig. 6 with a voltage-mode PWM and a proportional–integral controller. The circuit and controller parameters are: $R_1 = 0.1\ \Omega$, $L_1 = 100\ \mu$H, $C_1 = 200\ \mu$F, $R_2 = 20\ \Omega$, $k_p = 0.1$, $k_i = 400$, $i_{\max} = 5$ A, $e_o = 10$ V, $e_{\sigma_1} = 15$ V and $e_{\sigma_2}$ is a sawtooth with unitary amplitude and frequency $1/T_c = 5$ kHz. The closed-loop power converter can be modeled in the form (17) with the matrices given by (28). Such model is valid for all operating conditions (continuous and discontinuous conduction modes) of the power converter. A periodic solution of period $T_c$ is expected.

By discretizing the system with $N_h = 130$ samples per period, which corresponds to $h = 1.53\ \mu$s, we can construct the mixed LC problem (1) with the matrices defined in (30), (36), and (42). Figure 11 shows the

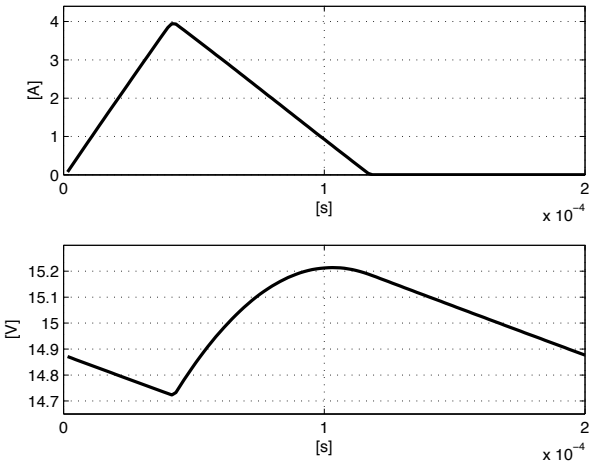


Fig. 11. Steady-state inductor current and output voltage computed by the LC procedure for the closed-loop boost DC–DC converter in discontinuous conduction mode.

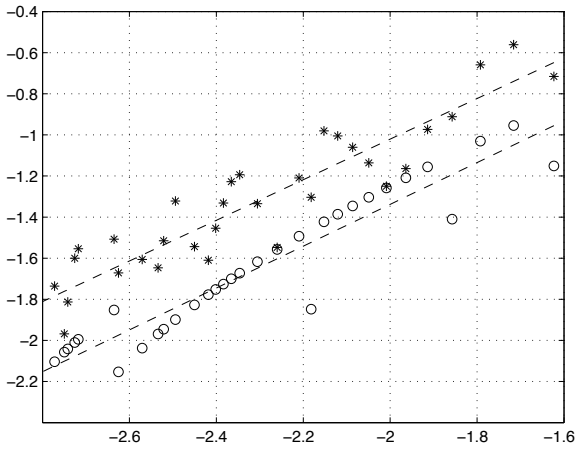

Fig. 12. Error in the trajectory computation obtained by varying $N_h \in [42, 642]$ for the closed-loop boost DC–DC converter in discontinuous conduction mode. The horizontal axis is $\log_{10}(1/N_h)$ and the vertical axis is the $\log_{10} \max |x_{\text{oi,plecs}} - x_{\text{oi}}|$ with $i = 1$ (*) and $i = 2$ (o). The dashed lines are the linear least square interpolations.

solutions obtained through the LC procedure. The computation time required to solve the mixed LC problem is $1.06$ s. The results show that the proposed algorithm is able to detect the steady-state behavior of the closed-loop converter operating in discontinuous conduction mode, which is a situation difficult to be a priori predicted without introducing some simplifying assumptions. Figure 12 shows that the maximum error decreases when $N_h$ increases, thus confirming the effectiveness of the proposed approach.

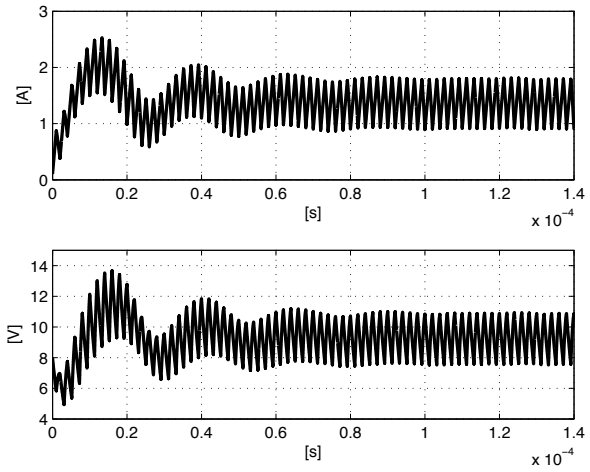


Fig. 13. Time evolution obtained with the time-stepping LC procedure for the closed-loop boost DC–DC converter.

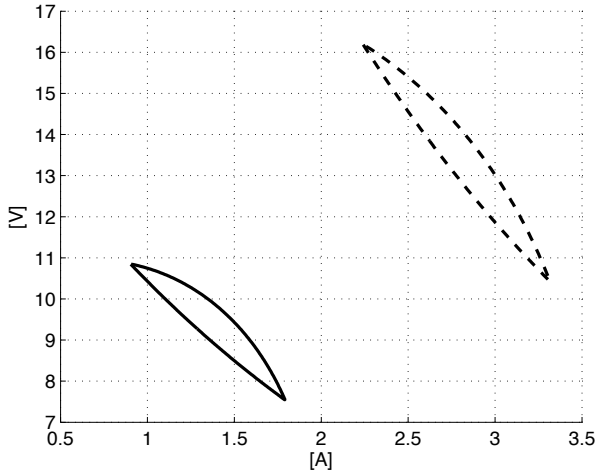


Fig. 14. Phase plane corresponding to the stable (continuous line) and the unstable (dashed line) solutions obtained with the LC technique applied to the closed-loop boost DC–DC converter.

The non-regularity of the computed error is mainly due to the chosen discretization technique. This phenomenon is generally observed when a high order method is used for a solution with limited smoothness, see [10, §9.1].

### *B. Boost converter with an unstable solution*

Consider the boost DC–DC converter shown in Fig. 6 with a PWM and a proportional controller whose scheme is in Fig. 7 where $y = k_1 x_{o_1} + k_2 x_{o_2}$, $e_{\sigma_1}$ is the reference output voltage and the integral term is zero, i.e., $k_i = 0$. This example shows that the LC approach is able to compute also unstable steady-state solutions. The matrices of

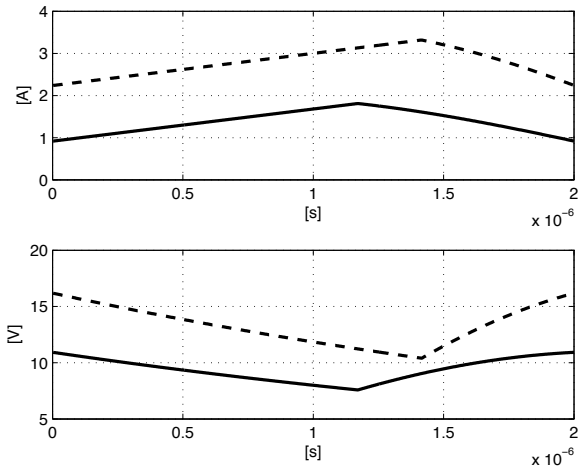


Fig. 15. Steady-state inductor current and capacitor voltage computed by solving the mixed LC problem described in Section IV and applied to the boost DC–DC converter: stable solution (continuous line) and unstable solution (dashed line).

the form (17) can be simply obtained by the procedure in Section III. The following parameters are used: $R_1 = 0\ \Omega$, $L_1 = 5.24$ µH, $C_1 = 0.2$ µF, $R_2 = 16\ \Omega$, $k_1 = -0.1$, $k_2 = 0.01$, $k_p = 1$, $i_{\max} = 5$ A, $e_o = 4$ V, $e_{\sigma_1} = 0.48$ V and $e_{\sigma_2}$ is a sawtooth with unitary amplitude and frequency $1/T_c = 500$ kHz.

In Fig. 13 it is depicted the time evolution of the stable solution obtained with the time-stepping numerical integration of the LC model and by choosing as initial conditions $x_{o_1} = 0.1$ A and $x_{o_2} = 8$ V. The results confirm those reported in [28].

In [28] it is shown that the closed-loop power converter exhibits two periodic solutions with period $T_c$: one stable and another unstable. Figure 14 shows the stable (continuous line) and the unstable (dashed line) solutions in the current–voltage plane obtained with the LC approach and $N_h = 400$, which corresponds to $0.005$ µs. The results are also coherent with those presented in [36]. The two solutions are obtained by using the PATH algorithm [30] with zero (nonzero) initial guess for the stable (unstable) solution. In Fig. 15 such steady-state signals have been plotted with respect to the time. The computation time is $2.04$ s for the stable solution and $2.06$ s for the unstable one.

### *C. Boost converter with current-mode control*

Consider the boost DC–DC converter in Fig. 6 under current-mode control with slope compensation. Because of the presence of a memory element, that is the flip-flop, it is opportune to formalize the current-mode control problem in the discrete-time domain. A corresponding block diagram is shown in Fig. 16, where $e_{\sigma_1}$ is the reference current value, $e_{\sigma_2}$ is the external compensation ramp, $e_{\sigma_3}$ is the clock signal that is 1 for one sample at the beginning of the period, i.e., $k = 1$ and it is zero for $k = 2, 3, \ldots, N_h$. The behaviour of the S-R flip-flop can be modeled by

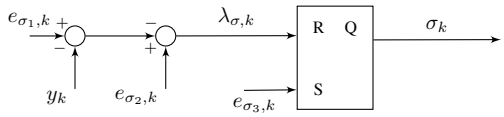


Fig. 16. Block diagram of the current-mode controller: $e_{\sigma_1}$ is the reference signal for the output variable $y$, that is a current; $e_{\sigma_2}$ is the compensation ramp; $e_{\sigma_3}$ is the clock; $\sigma$ is the switching signal.

using the following function

$$\sigma_k = 1 - (1 - e_{\sigma_3,k})\text{sat}_{[0,1]}(1 - \sigma_{k-1} + \text{step}(\lambda_{\sigma,k})) \tag{46a}$$

$$\lambda_{\sigma,k} = x_{o_1,k} - e_{\sigma_1,k} + e_{\sigma_2,k} \tag{46b}$$

where $\text{sat}_{[0,1]}$ is the saturation function between zero and one and step is the unitary amplitude step function, that we have already analyzed in Section III-B, see Fig. 3(b). For $k = 1$, the clock value $e_{\sigma_3,k}$, is set to 1 and from (46a) the control signal $\sigma$ is set to 1 independently on the value of the current (switch ON). The switch stays ON, i.e., $\sigma$ keeps the value 1, until the current $x_{o_1,k} = y_k$ reaches the compensation ramp $e_{\sigma_1,k} - e_{\sigma_2,k}$ for some value of $k$. At this value of $k$, $\lambda_{\sigma,k}$ becomes nonnegative and the output of the step function changes from 0 to 1. After that the control variable $\sigma$ is zero, i.e., the switch is OFF until the beginning of the next period also in the case $\lambda_{\sigma,k}$ changes again its sign. By replacing in (46a) the saturation and the step function with the corresponding complementarity representation, we obtain the complementarity model of the control signal in the case of current-mode control

$$\sigma_k = 1 - (1 - e_{\sigma_3,k})z_{\sigma_2,k} \tag{47a}$$

$$w_{\sigma_1,k} = -z_{\sigma_2,k} + 1 \tag{47b}$$

$$w_{\sigma_2,k} = z_{\sigma_1,k} + z_{\sigma_2,k} - z_{\sigma_3,k} - 1 + \sigma_{k-1} \tag{47c}$$

$$w_{\sigma_3,k} = z_{\sigma_4,k} - \lambda_{\sigma,k} \tag{47d}$$

$$w_{\sigma_4,k} = -z_{\sigma_3,k} + 1 \tag{47e}$$

$$0 \leqslant w_{\sigma,k} \perp z_{\sigma,k} \geqslant 0, \tag{47f}$$

where $\lambda_{\sigma,k}$ is given in (46b). By discretizing the open-loop LC model of the power converter in (19) and by considering (47) and the periodicity condition, the closed-loop discretized LC model in the form of (35) can be easily obtained. Consider the following parameters $R_1 = 0\ \Omega$, $R_2 = 22\ \Omega$, $C_1 = 880\ \mu\text{F}$, $L_1 = 69\ \mu\text{H}$, $i_{\max} = 10\ \text{A}$, $e_o = 16.9\ \text{V}$, $e_{\sigma_1} = 12.58\ \text{A}$ and $e_{\sigma_2}$ is the compensation ramp with slope equal to $8.4 \times 10^5\ \text{As}^{-1}$ and frequency $1/T_c = 100\ \text{kHz}$. Figure 17 shows the steady-state results obtained by applying the LC procedure. The results are coherent with the experimental results presented in [4].

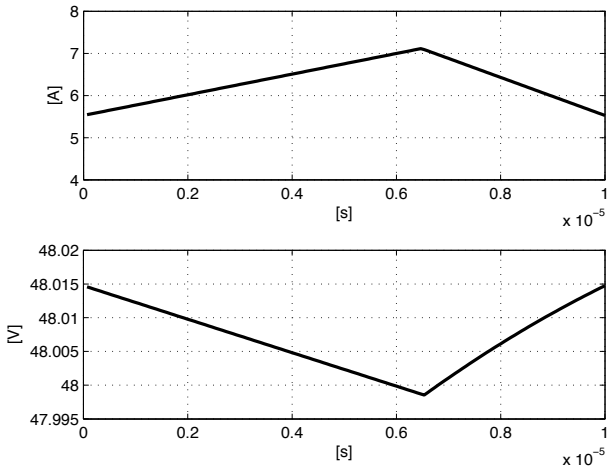


Fig. 17. Steady-state inductor current $x_{o_1}$ and capacitor voltage $x_{o_2}$ (continuous line) computed by using the LC procedure for the closed-loop boost DC–DC converter with current-mode control.

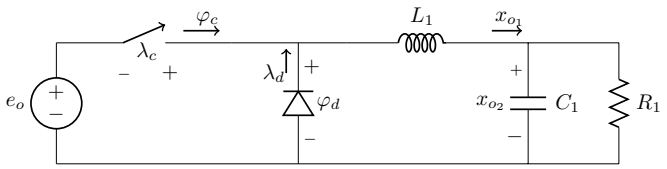


Fig. 18. Buck DC–DC converter.

### *D. Buck converter with period doubling bifurcation*

Consider the buck DC–DC converter shown in Fig. 18 with a voltage-mode PWM and a proportional controller whose scheme is in Fig. 7 where $y = k_1 x_{o_1} + k_2 x_{o_2}$, $e_{\sigma_1}$ is the reference output voltage and the integral term is zero, i.e., $k_i = 0$. In [29] it is shown that this power converter presents different kinds of bifurcations, under the variation of the input voltage $e_o$ and the frequency of the carrier signal $e_{\sigma_2}$. When the following parameters are chosen $R_1 = 22\ \Omega$, $C_1 = 47\ \mu\text{F}$, $L_1 = 5.8\ \text{mH}$, $k_p = 1$, $k_1 = 0.02$, $k_2 = 2$, $i_{\max} = 5\ \text{A}$, $e_o = 20\ \text{V}$, $e_{\sigma_1} = 8\ \text{V}$ and $e_{\sigma_2}$ is a sawtooth signal with a frequency $1/T_c = 1.013\ \text{kHz}$ and whose amplitude varies between $2.4\ \text{V}$ and $8\ \text{V}$, the buck DC–DC converter has a period doubling bifurcation. By using the procedure described in Section III, i.e., by appling the Kirchhoff laws to the circuit in Fig. 18 and by using (4), (7) and (22), the LC model of the

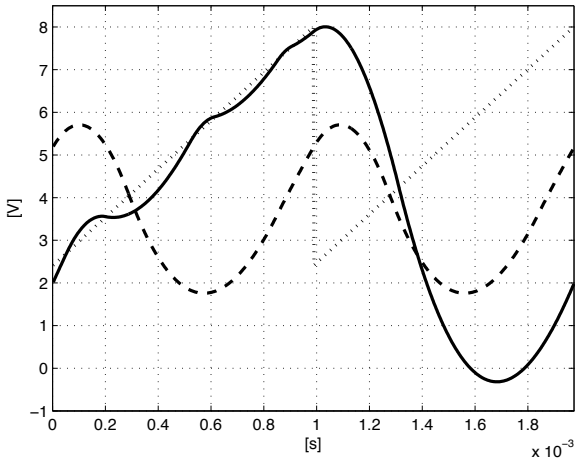


Fig. 19. Carrier signal $e_{\sigma_2}$ (dotted line) and modulation signals for stable double-period solution (continuous line) and single-periodic unstable solution (dashed line) for the closed-loop buck DC–DC converter.

closed-loop power converter can be written as follows

$$\dot{x}_{o_1} = -\frac{1}{L_1}x_{o_1} - \frac{1}{L_1}x_{o_2} + \frac{1}{L}z_d \tag{48a}$$

$$\dot{x}_{o_2} = \frac{1}{C_1}x_{o_1} - \frac{1}{C_1 R_1}x_{o_2} \tag{48b}$$

$$w_d = x_{o_1} - z_{c_1} \tag{48c}$$

$$w_{c_1} = z_d + z_{c_2} - e_o \tag{48d}$$

$$w_{c_2} = -z_{c_1} + i_{\max} z_{\sigma_1} \tag{48e}$$

$$w_{\sigma_1} = k_p x_{o_2} + z_{\sigma_2} - k_p e_{\sigma_1} + e_{\sigma_2} \tag{48f}$$

$$w_{\sigma_2} = -z_{\sigma_1} + 1 \tag{48g}$$

$$0 \leqslant w \perp z \geqslant 0 \tag{48h}$$

which is in the form (17) with $x = \mathrm{col}(x_{o_1}, x_{o_2})$, $z = \mathrm{col}(z_d, z_{c_1}, z_{c_2}, z_{\sigma_1}, z_{\sigma_2})$, $w = \mathrm{col}(w_d, w_{c_1}, w_{c_2}, w_{\sigma_1}, w_{\sigma_2})$ and $e = \mathrm{col}(e_o, e_{\sigma_1}, e_{\sigma_2}, 1)$. The converter has an unstable solution with the same period of the sawtooth and a stable steady-state solution with double-period, that is $T = 2T_c$.

By discretizing the system with $N_h = 350$ samples ( $h = 5.6$ µs for the unstable solution and $h = 2.8$ µs for the stable one) and by constructing the mixed LC problem (1) with the matrices defined in (30), (36) and (42), the PATH algorithm with zero and nonzero initial guesses provides the solutions shown in Fig. 19 and Fig. 20.

Figure 21 shows the comparison between the numerical results obtained with the complementarity procedure and the experimental results presented in [29] and confirms the effectiveness of the proposed approach. In the same figure, with the dash-dotted line we present also the solution characterized by sliding motion obtained by setting

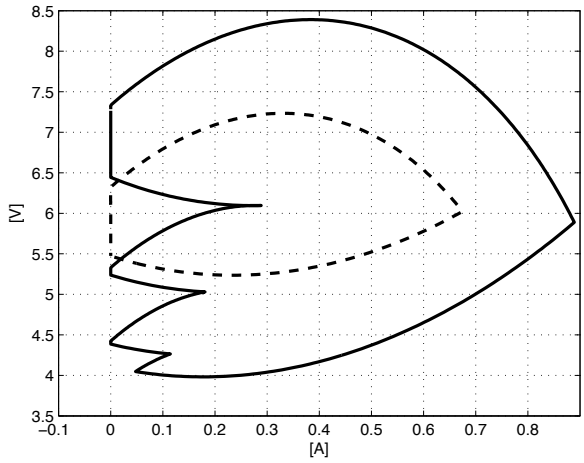


Fig. 20. Phase plane corresponding to the different solutions of the closed-loop buck DC–DC converter in Fig. 19: unstable (dashed line) and stable (continuous line). Note the presence of multiple discontinuous conduction mode phases during the double-periodic solution.

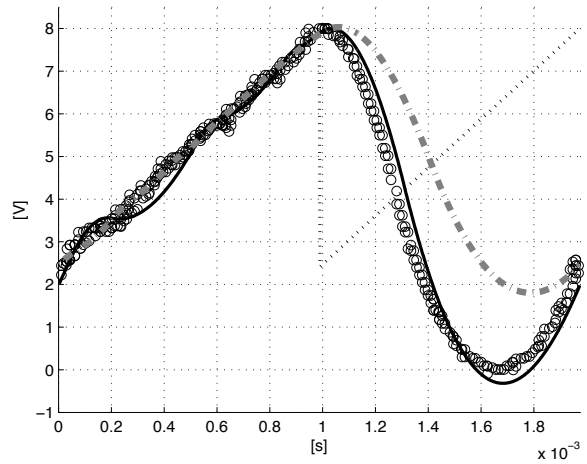


Fig. 21. Comparison with experimental results (dots) for the closed-loop buck DC–DC converter: carrier signal $e_{\sigma_2}$ (dotted line) and simulation solution (continuous line). Numerical solution with sliding motion (dot-dashed line) obtained with different control parameters.

the value of the reference voltage $e_{\sigma_1} = 12$ V and the control parameters $k_1 = 0.01$ and $k_2 = 1.05$.

## VII. Conclusions

Linear complementarity (LC) systems are an interesting class of models suitable for the representation of the dynamic evolutions of power converters. One of the major drawbacks of the LC models previously proposed in the literature for power converters was the presence of switched sets (cones) required for the representation of the switches characteristics. That made very complicated the construction of complementarity models for controlled converters. The LC model proposed in this paper for the voltage–current piecewise linear characteristics of switches

allows to represent power converters as non-switched LC systems. The LC model structure with constant matrices is valid for both open-loop and closed-loop power converters, and it can be obtained by combining the dynamical equations describing the circuit with the LC representations of the electronic devices, modulator and controller. The LC model can be used for the time-stepping evolution and for the steady-state oscillation computations. In particular, the steady-state solution of the discretized closed-loop system has been formulated as the solution of a static mixed LC problem. The proposed technique has been shown to be effective for the computation of the transient and the steady-state periodic oscillations exhibited by closed-loop Z-source, boost and buck DC–DC power converters operating in continuous or discontinuous conduction mode and also in the presence of multiple solutions.

Future work will be dedicated to improve the numerical effectiveness of the LC model integration, to the order model reduction issue within the complementarity framework and to the application of the proposed technique for the analysis of more complex nonlinear phenomenon in switched circuits.

## REFERENCES


[1] B. De Kelper, L. A. Dessaint, K. Al-Haddad, and H. Nakra, "A comprehensive approach to fixed-step simulation of switched circuits," *IEEE Trans. Power Electron.*, vol. 17, no. 2, pp. 216–224, 2002.

[2] R. W. Erickson and D. Maksimovic, *Fundamentals of Power Electronics*, 2nd ed. Kluwer Academic Publishers, 2001.

[3] D. Maksimovic, A. M. Stankovic, V. J. Thottuvelil, and G. C. Verghese, "Modeling and simulation of power electronic converters," *IEEE Power Electronics Specialists Conf. Rec.*, vol. 89, no. 6, pp. 898–912, 2001.

[4] T. Pavlovic, T. Bjazic, and Z. Ban, "Simplified averaged models of dc-dc power converters suitable for controller design and microgrid simulation," *IEEE Trans. Power Electron.*, vol. 28, no. 7, pp. 3266–3275, 2013.

[5] H. Peng, A. Prodic, E. Alarcon, and D. Maksimovic, "Modeling of quantization effects in digitally controlled DC–DC converters," *IEEE Trans. Power Electron.*, vol. 22, no. 1, pp. 208–215, 2007.

[6] A. Davoudi, J. Jatskevich, and T. De Rybel, "Numerical state-space average-value modeling of PWM DC–DC converters operating in DCM and CCM," *IEEE Trans. Power Electron.*, vol. 21, no. 4, pp. 1003–1012, 2006.

[7] R. Cottle, J. Pang, and R. Stone, *The linear complementarity problem*, 2nd ed. Boston, MA: Academic Press, 2009.

[8] M. K. Camlibel, W. P. M. H. Heemels, A. J. v. der Schaft, and J. M. Schumacher, "Switched networks and complementarity," *IEEE Trans. Circuits Syst. I*, vol. 50, no. 8, pp. 1036–1046, 2003.

[9] V. Acary, O. Bonnefon, and B. Brogliato, "Time-stepping numerical simulation of switched circuits within the nonsmooth dynamical systems approach," *IEEE Trans. Computer-Aided Design of Integrated Circuits and Systems*, vol. 29, no. 7, pp. 1042–1055, 2010.

[10] V. Acary and B. Brogliato, *Numerical methods for nonsmooth dynamical systems*. Berlin Heidelberg: Springer-Verlag, 2008, vol. 35.

[11] V. Sessa, L. Iannelli, V. Acary, B. Brogliato, and F. Vasca, "Computing period and shape of oscillations in piecewise linear lur'e systems: a complementarity approach," in *IEEE Conference on Decision and Control*, Florence, Italy, dec. 2013.

[12] F. Vasca, L. Iannelli, M. K. Camlibel, and R. Frasca, "A new perspective for modeling power electronics converters: complementarity framework," *IEEE Trans. Power Electron.*, vol. 24, no. 2, pp. 456–468, 2009.

[13] V. Acary, O. Bonnefon, and B. Brogliato, *Nonsmooth Modeling and Simulation for Switched Circuits*. London, U.K.: Springer-Verlag, 2011.

[14] J. J. Rico-Melgoza, J. P. Suarez, E. Barrera-Cardiel, and M. M. Martinez, "Modeling and analysis of three-phase diode bridge rectifiers as linear complementarity systems," *Electric Power Components and Systems*, vol. 47, no. 15, pp. 1639–1655, 2009.

[15] G. Angelone, F. Vasca, L. Iannelli, and K. Camlibel, "Dynamic and steady-state analysis of switching power converters made easy: Complementarity formalism," in *Dynamics and Control of Switched Electronic Systems*, F. Vasca and L. Iannelli, Eds. London, U.K.: Springer-Verlag, 2012.

[16] L. Iannelli, F. Vasca, and G. Angelone, "Computation of steady–state oscillations in power converters through complementarity," *IEEE Trans. Circuits Syst. I*, vol. 58, no. 6, pp. 1421–1432, 2011.

[17] C. Batlle, E. Fossas, I. Merillas, and A. Miralles, "Generalized discontinuous conduction modes in the complementarity formalism," *IEEE Trans. Circuits Syst. II*, vol. 52, no. 8, pp. 447–451, 2005.

[18] N. Carrero, C. Batlle, and E. Fossas, "Modeling a coupled-inductor boost converter in the complementarity framework," in *6th UKSim/ AMSS European Symposium on Computer Modeling and Simulation*, Valletta, Malta, nov. 2012, pp. 471–476.

[19] J. Tant, J. Driesen, and W. Michiels, "Event-driven simulation of power electronics in the complementarity systems framework," in *IEEE 13th Workshop on Control and Modeling for Power Electronics*, Kyoto, Japan, jun. 2012, pp. 1–7.

[20] C. Glocker, "Models of non-smooth switches in electrical systems," *Int. J. Circ. Theor. App.*, vol. 33, no. 3, pp. 205–234, 2005.

[21] D. Goeleven, "Existence and uniqueness for a linear mixed variational inequality arising in electrical circuits with transistor," *J. Optim. Theory Appl.*, vol. 138, pp. 397–406, 2008.

[22] M. Shirazi, R. Zane, and D. Maksimovic, "An autotuning digital controller for DC-DC power converters based on online frequency-response measurement," *IEEE Trans. Power Electron.*, vol. 24, no. 11, pp. 2578–2588, 2009.

[23] R. Yang, H. Ding, Y. Xu, L. Yao, and Y. Xiang, "An analytical steady-state model of LCC type series-parallel resonant converter with capacitive output filter," *IEEE Trans. Power Electron.*, vol. 29, no. 1, pp. 328–338, 2014.

[24] K. Ilves, A. Antonopoulos, S. Norrga, and H.-P. Nee, "Steady-state analysis of interaction between harmonic components of arm and line quantities of modular multilevel converters," *IEEE Trans. Power Electron.*, vol. 27, no. 1, pp. 57–68, 2012.

[25] Q. Song, W. Liu, X. Li, H. Rao, S. Xu, and L. Li, "A steady-state analysis method for a modular multilevel converter," *IEEE Trans. Power Electron.*, vol. 28, no. 8, pp. 3702–3713, 2013.

[26] R. Yu, G. K. Y. Ho, B. M. H. Pong, B.-K. Ling, and J. Lam, "Computer-aided design and optimization of high-efficiency LLC series resonant converter," *IEEE Trans. Power Electron.*, vol. 27, no. 7, pp. 3243–3256, 2012.

[27] V. P. Galigekere and M. K.Kazimierczuk, "Small-signal modeling of open-loop PWM Z-source converter by circuit-averaging technique," *IEEE Trans. Power Electron.*, vol. 28, no. 3, pp. 1286–1296, 2013.

[28] J. W. van der Woude, W. L. de Koning, and Y. Fuad, "On the periodic behavior of PWM DC–DC converters," *IEEE Trans. Power Electron.*, vol. 17, no. 4, pp. 585–595, 2002.

[29] M. Di Bernardo, F. Garofalo, L. Iannelli, and F. Vasca, "Bifurcations in piecewise-smooth feedback systems," *International Journal of Control*, vol. 75, no. 16-17, pp. 1243–1259, 2002.

[30] S. P. Dirkse and M. C. Ferris, "The PATH solver: a non-monotone stabilization scheme for mixed complementarity problems," *Optim. Methods Softw.*, vol. 5, pp. 123–156, 1995.

[31] L. Han, A. Tiwari, M. K. Camlibel, and J.-S. Pang, "Convergence of time-stepping for passive and extended linear complementarity systems," *SIAM J. Numer. Anal.*, vol. 47, no. 5, pp. 3768–3796, 2009.

[32] R. Frasca, M. K. Camlibel, I. C. Goknar, L. Iannelli, and F. Vasca, "Linear passive networks with ideal switches: Consistent initial conditions and state discontinuities," *IEEE Trans. Circuits Syst. I*, vol. 57, no. 12, pp. 3138–3151, 2010.

[33] V. P. Galigekere and M. K.Kazimierczuk, "Analysis of PWM Z-source DC–DC converter in CCM for steady state," *IEEE Trans. Circuits Syst. I*, vol. 59, no. 4, pp. 854–863, 2012.

[34] L. Iannelli and F. Vasca, "Computation of limit cycles and forced oscillations in discrete time piecewise linear feedback systems through a complementarity approach," in *IEEE Conference on Decision and Control*, Cancun, Mexico, dec. 2008, pp. 1169–1174.

[35] [Online]. Available: http://www.plexim.com/

[36] C. C. Fang, "Critical conditions of saddle-node bifurcations in switching DC–DC converters," *International Journal of Electronics*, vol. 100, no. 8, pp. 1–28, 2012.